

# Spectrum of genetic diversity and networks of clonal plant populations

Alejandro F. Rozenfeld\*, Sophie Arnaud-Haond†, Emilio Hernández-García\*, Víctor M. Eguílez\*, Manuel A. Matías\*, Ester Serrão† and Carlos M. Duarte§

\* Cross-Disciplinary Physics Department, IMEDEA (CSIC-UIB), Instituto Mediterráneo de Estudios Avanzados, Campus Universitat de les Illes Balears, 07122 Palma de Mallorca, Spain

† CCMAR, CIMAR-Laboratório Associado, Universidade do Algarve, Gambelas, 8005-139, Faro, Portugal

§ Natural Resources Department, IMEDEA (CSIC-UIB), Instituto Mediterráneo de Estudios Avanzados, C/ Miquel Marques 21, 07190 Esporles, Mallorca, Spain

## Abstract

Clonal organisms present a particular challenge in population genetics because, in addition to the possible existence of replicates of the same genotype in a given sample, some of the hypotheses and concepts underlying classical population genetics models are indeed irreconcilable with clonality. The genetic structure and diversity of clonal plant populations was examined using a combination of new tools to analyze microsatellite data in the marine angiosperm *Posidonia oceanica*. These tools were based on examination of the frequency distribution of the genetic distance among ramets, termed the spectrum of genetic diversity (GDS), and of networks built on the basis of pairwise genetic distances among genets. Clonal growth and outcrossing are apparently dominant processes, whereas selfing and somatic mutations appear to be marginal, and the contribution of regular immigration from distant populations seems to play a small role in adding genetic diversity to populations. The properties and topology of networks based on genetic distances showed that populations follow a “small-world” topology, characterized by a high degree of connectivity among nodes, and a high hierarchical substructure, revealing a structure in sub-families of closely related individuals. The combination of GDS and network tools proposed here helped in dissecting the influence of various evolutionary processes in shaping the intra-population genetic structure of the clonal plant investigated; these therefore represent promising alternative analytical tools in evolutionary ecology.

## Introduction

The considerable progress achieved during the last decades in molecular biology and biotechnologies has greatly enhanced the potential of molecular markers for studying the process of evolution in natural populations in the framework of population genetics. As the empirical basis for population genetics is broadened, it is increasingly clear that the theoretical constructs under which population analyses are traditionally conducted involve assumptions that are often violated in natural scenarios, such as the random mating, equilibrium (1), and non-overlapping generations commonly assumed for interpreting statistics on population genetic composition and structure (2).

The summary statistics used in population genetics to estimate relevant parameters such as departure from panmixia or the population structure indeed rely on theoretical and mathematical models that involve the adoption of a somewhat narrow range of underlying parameters and demographic models; this greatly limits the scope of demographic situations that can be accurately explored (2). Among others, two examples in which the assumptions underlying the classical Wright-Fisher model (1) of population genetics are violated are the cases of endangered and invasive species. These are among the type of species most studied in evolutionary ecology, precisely because they exhibit population dynamics that strongly depart from equilibrium, which very much limits the interpretation of classical population genetics statistics. These constraints on the application of conventional metrics of population genetic structure are even more evident for clonal organisms, the characteristics of which challenge the notions of effective population size and generation time (3, 4). Moreover, a clear concept of the unit (genetic individual) on which evolutionary forces are acting is lacking (5, 6) for clonal species.

Examination of the genetic structure of populations is rooted in a comparison of the extent of genetic variability among individuals within populations, as well as differences among the populations, typically assessed using appropriate molecular markers applied to statistically-representative samples of individuals. Hypervariable markers such as microsatellites are commonly considered to be the markers of choice in assessing the genetic variability and structure of populations. This is particularly true in the case of clonal organisms, for which they allow, in a given sample, proper assessment of the individual level through the isolation of distinct multi-locus genotypes or lineages, which is a prerequisite for estimating variability and structure in clonal populations. Furthermore, most evaluations of genetic composition of clonal (and non-clonal) populations are based on summary statistics, such as heterozygosity or fixation indices, that do not consider the distribution of genetic distances among the sampled individuals. In fact, metrics to assess these distances are surprisingly scarce (7, 8).

The depiction of a population structure as a concerted representation of the genetic distances between agents (individuals or ramets in clonal species) implies that examination of the genetic structure of populations as a network, in which the links between agents depend on the genetic difference between them, is a suitable approach. Such a representation suggests that network analysis is an additional effective tool for examining the genetic structure of organisms and formulating diagnostics for the underlying processes. The use of networks to graphically represent genetic relationships has emerged as a useful tool in cases in which the nodes are haplotypes (9–14) or populations (15). Here we propose a network representation of the genetic structure of clonal plant populations focused on the ramet as the interacting agents. We represent the intra-population genetic similarities among the genetic individuals in clonal plant populations as networks. In addition, we go one step further from the simple graphical representation of genetic relationships, and quantitatively analyze the properties of the resulting networks using tools (see Methods) successfully applied to other problems (16), such as the characterization of food webs (17, 18) and the analysis of protein (19) or gene (20) interactions.

We demonstrate this approach using a clonal seagrass species (*Posidonia oceanica*) for which a large data set, including microsatellite data for approximately 1500 shoots sampled from 37 populations across the Mediterranean, is available. We first propose a metric for genetic distances among individuals based on their observed multi-locus microsatellite genotypes, which allows us to describe the spectrum of genetic diversity within populations. We then explore the biological processes that yield the observed spectra, and use this knowledge to topologically represent the population as a network, from which structural diagnostics are then derived.

## Results and discussion

### Genetic diversity spectrum

The meadows sampled differed greatly in clonal diversity, ranging from highly clonal (e.g., Es Castell, Spain,  $R=0.10$ ) to highly diverse (e.g., Calabardina, Spain,  $R=0.88$ ; Table 2, which is published as Supplementary information on the PNAS web site). The genetic distance between pairs of individuals within any population ranged from  $D=0$  for clonal mates, to as much as  $D=200$  for the most genetically divergent individuals present in any population. The distribution of  $D$  within any population is represented as a frequency distribution of all pairwise values, which we refer to as the *Genetic Diversity Spectrum* (GDS) of each population. The GDS is analogous to the frequency distribution of pairwise differences used on some clonal organism to detail the influence of clonality, as well as possible somatic mutations or scoring errors (7, 8, 21). Nevertheless, we propose here to extend its interpretation beyond that particular application, using simulations to screen for the influence of some of the evolutionary forces that can contribute to shape the pattern of genetic diversity at the intra-population scale. In particular, we examine the importance of the mating system (outcrossing, selfing), which influences the way alleles are transmitted from one generation to the next, thereby playing a central role in the changing of allele frequencies across generations.

The GDS of the populations studied showed a range of shapes across populations (Fig. 1 and Fig. 5, which is published as supporting information on the PNAS web site). Three of the populations sampled (namely, Es Castell, Cala Fornells and Es Port) showed spectra indicative of a strongly clonal composition, characterized by a large spike at zero distance corresponding to the null distance between ramets pertaining to the same genetic individual, and discrete peaks located at characteristic genetic distances between the few distinct clones present in the population (Fig. 1a). Most of the populations sampled, however, are characterized by a broad, bimodal GDS (e.g., Fig. 1b), with a smaller (and broader) mode at zero distance, indicating the existence of nearly identical individuals forming clones, and a mode at higher distances within a broad, skewed, bell-shaped distribution.

The characteristic features of the GDS of *P. oceanica* populations were highlighted by producing the average GDS across all sampled populations ( $\langle \text{GDS} \rangle$ , Fig. 2). The resulting  $\langle \text{GDS} \rangle$  is strongly bimodal, showing a large peak at 0 distance ( $\alpha$  peak), suggesting that clonal reproduction constitutes one of the main factors influencing the intra-population genetic structure. The  $\alpha$  peak

is followed, at small genetic distances, by a depression, indicating that low genetic distances between 4 and 12 nucleotides (nt) are uncommon. A broad peak ( $\beta$  peak) at a modal pairwise genetic distance of approximately 30 nt represents the most commonly observed genetic distances between genetically dissimilar (i.e., non-clonal) units sampled within populations. Above the  $\beta$  peak distance, the frequency of distances between individuals declines exponentially (Fig. 2). Provided that enough polymorphic loci are used (22), the process responsible for generating genetic distances of 0 among individuals can be unambiguously assigned to clonal reproduction. In contrast, the processes generating specific classes of greater genetic distances are less apparent. However, this knowledge is essential for understanding, from a biological and mechanistic point of view, the implications of the observed  $\langle GDS \rangle$  on the prevalence of various mechanisms that generate genetic diversity and structure within the population. The simulations performed allowed us to explore the range of genetic distances between parents and offspring, depending on the reproductive mode. The mean, across the populations examined, simulated genetic distance ( $\pm SE$ ) generated by selfing and outcrossing was  $13.8 \pm 1.1$  and  $24.0 \pm 1.2$ , respectively (Fig. 2). The characteristic genetic distance generated by simulated outcrossing ( $\delta_{oc} = \delta^{(1)}_{oc}$ ) is remarkably close to the modal  $\beta$  peak of the  $\langle GDS \rangle$  (Fig. 2), suggesting that outcrossing is the main mechanism generating genetic diversity within the populations of this species. In contrast, the characteristic genetic distance generated by selfing ( $\delta_s$ ) is located at the edge of the depression between the  $\alpha$  and  $\beta$  peaks in the  $\langle GDS \rangle$ , implying a low contribution of selfing in generating genetic distances in the meadows, and therefore a limited rate of selfing compared to outcrossing and clonality.

Observation of the  $\langle GDS \rangle$  also suggests that caution should be exercised when interpreting the valley between the  $\alpha$  and  $\beta$  peaks in the spectrum of genetic distances in terms of somatic mutations or scoring errors, as proposed for obligatory outcrossing species (8, 21), when dealing with possibly self-fertilizing species. A small genetic distance can also possibly be generated by selfing, a possibility that should be considered along with the more likely explanation that these distances arise from somatic mutations or scoring errors. In the case of possible self-fertilizers, simulations may be useful in defining the range of distances that can be generated sexually and the threshold below which clonality may be assumed. After such simulations in the case of *P. oceanica*, the uncommon distances between 2 and 6 are still unlikely (data not shown) under a mixed mating system, with the selfing rate not exceeding the proportion expected on the basis of clone size (in terms of the number of shoots). Since we are confident that the double-checking procedure applied to the first data set allowed the correction of most scoring errors, these small distances must be mostly generated by somatic mutations accumulated in the process of multiple clonal reproductive events. Indeed, *P. oceanica* clones are extremely long-lived, with clones dated to millennia (23), over which clones would have divided multiple times, hence providing opportunities for somatic mutations. Indeed, the frequency of individuals at distances between strictly clonal ( $D=0$ ) and the minimum observed in between the  $\alpha$  and  $\beta$  peaks ( $D=10$ ) also declines sharply, as expected from the low probability of accumulated mutations.

Lastly, the mean genetic distances from ancestors to offspring located  $n$  generations apart, obtained from simulations, increase very slowly with  $n$ , reaching an asymptote after eight generations (Fig. 3). Comparison between the largest distances obtained by simulations and those observed on the  $\langle GDS \rangle$  shows that the end of the distribution tail is not likely to be accounted for by either outcrossing or mutation. These distances are not likely to be generated by the random rearrangement of alleles during outcrossing over generations, but rather by external factors that generate diversity. The most likely process is a very low rate of immigration from other populations, which can suddenly introduce individuals genetically very distinct from those present in the population. However, examination of the contribution of immigration requires GDS evaluation across the entire distribution range of the species, rather than population-specific analyses such as that presented here.

#### Network representation of the GDS

The discussion above indicates that the GDS is best conceptualized as the result of genetic exchanges among a network of individual genets. Network analysis may, thus, provide a step forward in topologically characterizing the genetic relationships between population constituents depicted in the GDS. A first step to construct such network is to define the threshold genetic distance ( $D_{th}$ ) representing closely genetically-connected individuals, characterized by between-individual distances  $\leq D_{th}$ . Based on analysis of the GDS, we elected to represent  $D_{th}$  by the one-generation outcrossing distance, which approximately corresponds to the  $\beta$  peak in the GDS of each population (i.e.,  $D_{th} = \delta_{oc}$ ). The network resulting from the connection of individuals at distances  $\leq D_{th}$  represents the links among individuals that are approximately *up to a generation apart*, on the understanding that the genetic distance is only an operational proxy for the kinship among the individuals. Networks in which nodes are either individual ramets or genetic individuals (i.e., different genets) have both been constructed. In the following we show the results for networks of genets, since the structure of ramet networks was straightforwardly obtained from them. The networks representing *P. oceanica* populations differ greatly in shape (Fig. 4), describing highly contrasting network properties across the meadows analyzed. The highly clonal population appears as a simple diagram of separate families with two or more clones each (Fig. 4a). In contrast, the network corresponding to the more diverse population is readily characterized by greater connectivity, showing a number of closely connected groups (sub-families) linked together by connections to a small set of central individuals, which act as links connecting the different families (Fig. 4b,d,e). In addition, we can distinguish fragmented (Fig. 4c) from fully connected (Fig. 4f) networks. There is an interesting parallel between the sub-structure revealed by the network shapes and the occurrence of spatial autocorrelation in some meadows (Cala Jonquet, Acqua Azzura 5; Fig. 4). Indeed, autocorrelation is used to detect patterns of limited dispersion revealed by a significant relationship between genetic and geographic distance, but a significant pattern primarily implies a sub-structure of the population in families of closely related individuals. This is very clearly illustrated by the shape of the networks, particularly in meadows where a strong pattern was detected, such as Cala Jonquet (Fig. 4b), where two subfamilies of five and nine highly interconnected individuals are linked together by a tiny path of three links and two intermediate nodes/individuals. However, failure to detect significant autocorrelation does not imply the absence of sub-families in the population, but only a lack of relationship between this genetic structure and geographic distance, or else low statistical power. Exploration of the network of individuals can therefore reveal the existence of a sub-structure of the meadows in various families, if it exists, even when no pattern of spatial autocorrelation can be detected.

The networks (examples in Fig. 4) constructed on the basis of the GDS spectra (Supplementary material, Fig. 5) for the *P. oceanica* populations differ greatly in properties (Table 1). The largest component,  $S$ , of each network contains most of the individuals of each meadow (Table 1), indicating that most of the individuals have at least another sampled individual in the meadow less than a generation apart (i.e.,  $\leq \delta_{oc}$ ). The average degree of network connectivity  $\langle k \rangle$  also differs greatly among populations (from

1.20 to 8.74, Table 1), with an overall average connectivity degree of 5.11, indicating that each individual is connected to, on average, five others. To indicate the significance of these numbers, we note that from the data in Table 1 the quantity  $\langle k \rangle / (G-1)$ , which is the average proportion of the genet population connected to a given individual, ranges between 0.13 and 0.55. This implies that each individual is separated by at most one average generation from between 13% and 55% of the individuals in the sample. Together with the average link density, this shows that a large number of links are already present in the networks at the threshold chosen. Indeed, the density of links in the network averages 27% (Table 1), indicating that two randomly selected individuals in a given population have a 27% probability of being less than one generation apart.

The average genetic connectivity of *P. oceanica* individuals (0.27; Table 1) is much higher than observed in other complex networks analyzed in the literature (24). Similarly, the clustering coefficient  $C$  (0.73; Table 1) is larger than observed in most reported networks. This value has to be compared with the clustering of an equivalent random network  $C_r$  containing the same number of nodes and links (see Methods).  $C$  is generally larger in the *P. oceanica* populations studied than the clustering expected if the network were random (i.e.,  $C > C_r$ , Table 1). This departure from a random network signals the presence of an important hierarchical genetic structure within the meadows at the level of closely related families, a pattern revealing low dispersal and family structure that often escapes analysis using classical autocorrelation estimations because of low statistical power or the absence of correlation with geographic distance. The average path length ( $L$ ), representing the minimum number of reproductive events or somatic mutations necessary to connect any two individual genets in the population, ranged from 1.00 to 3.44, averaging 1.88 across populations (Table 1). This average path length suggests that most ramets have a high kinship, typically below that of cousins, and is comparable to that generated by a random network. Taken together, the presence of short path lengths  $L \approx L_r$  and of higher than expected clustering coefficient  $C > C_r$  indicate that the networks of genetic relationships in *P. oceanica* populations have the characteristics of a small world (25). Small-world networks, as described extensively in the social sciences, characterize complex systems in which the connectivity range is not confined to a particular scale, and every node can be reached from every other using a small number of intermediate steps. This is indicative of a high degree of hierarchical genetic structure within populations of *P. oceanica*.

### Conclusions

The results presented here illustrate a novel approach, based on examination of the spectrum of genetic diversity, to examine the population genetic structure of clonal organisms and for the depiction of inter-individual genetic distances by a network. As underlined by Dyer and Nason (15), there are two fundamental distinctions between the classical genetic summary statistics that involve decomposing variance and the use of graphs. In the latter case, we do not impose pre-defined hierarchical models that constrain the range of temporal scales and evolutionary processes that can be accurately screened, but rather take advantage of all the information contained in the data set to let the data define their own topology and eventually offer a visual illustration. Here, we went one step further than graphical illustration by detailing the network properties using statistical tools specific to network analyses to extract key information on the hierarchical genetic structure in the population studied. This approach can be extended to explore the genetic structure of virtually any populations beyond the species case of a marine clonal plant examined here. In doing so, many new elements have been introduced, such as a parsimony metric of distance among individual diploid organisms, the basis for the construction of the spectrum of genetic diversity. We also used simple simulations to explore the partition of the contribution of different processes to the genetic diversity contained in the spectrum, and topological representations of networks of genetic relationships derived from the spectrum of genetic diversity to formally explore the properties of the resulting network. Each of these novel approaches is rooted in earlier developments in different fields, such as computational population genetics (7), population genetics (15, 26), and network analysis developed in the realm of complex-systems theory (24, 25, 27), but are brought together here to provide a synthetic parsimony analysis of population genetic structures.

This interdisciplinary effort has allowed us to derive key features of the population genetics of the clonal plant studied, such as the low contribution of somatic mutations and selfing to genetic diversity, and the inference, derived from examination of the spectrum of genetic diversity and subsequent network analysis, that *P. oceanica* populations show a rather high kinship level and low imports of propagules produced in other populations. The network illustration allowed us to underline the high degree of sub-structure in some meadows, clearly composed of several families. The analysis of network properties allowed us to describe *P. oceanica* populations as following a typical “small-world” network shape, a feature already widely described in complex systems such as the World Wide Web and social networks (26), characterized by small diameters and hierarchical structure leading to large clustering. The analysis of multiple populations has allowed elucidation of the considerable variability in the spectra of genetic diversity among populations, while identifying characteristic features in the spectrum. The results presented here reveal the spectral and network analysis of genetic diversity as a promising tool to ascertain the genetic structure of populations and the role of different processes in shaping it.

## Methods

### Model species

*Posidonia oceanica* is a clonal marine angiosperm restricted to the Mediterranean Sea, where it develops extensive meadows ranging from 0 to 40 m in depth (23). It is a very slow-growing organism, with the clones extending horizontally through the growth of rhizomes at approximately 2 cm year<sup>-1</sup>, developing shoots (ramets, the individual module repeated to develop clones) at intervals of approximately 5–10 cm. This monecious species (i.e., both male and female flowers on the same shoot) (23) is characterized by sparse episodes of sexual reproduction. Individual *P. oceanica* shoots (ramets) live for up to 50 years, and the clones have been aged to over 1000 years (23). The plants are experiencing basin-wide decline and are subject to specific protection and conservation measures (28–30).

### Multi-locus microsatellite genotypes

Approximately 40 *P. oceanica* shoots were sampled in each of 37 localities ranging, from west to east, from the Spanish Mediterranean Coast to Cyprus (Table 2, Supplementary information), encompassing a distance range of approximately 3500 km. In all meadows, shoots were collected at randomly drawn coordinates across an area of 20 m × 80 m. Then a meristem portion of each shoot was removed, desiccated and preserved in silica crystals.

Genomic DNA was isolated following a standard CTAB extraction procedure (31). The 37 meadows were analyzed with the most efficient combination (22, 32) of seven nuclear markers, using the conditions described by Arnaud-Haond et al. (22, 32). This set of microsatellite markers allows the unambiguous identification of clonal membership (22).

To avoid scoring errors, which would typically generate very small apparent genetic dissimilarities among individuals actually sharing the same multi-locus microsatellite genotype and would thus affect our estimates of genetic distance, all ramets with a distinct genotype for only two or one alleles were re-genotyped for those loci to ascertain their dissimilarity or to correct for genotyping errors. The clonal or genotype diversity was estimated as  $R=(G-1)/(N-1)$ , where  $G$  is the number of genotypes discriminated and  $N$  is the number of samples analyzed.

### Similarity metrics

To characterize the genetic structure of the different populations, some measure of genetic similarity among ramets is needed. Whereas there are multiple choices for similarity metrics among populations, and between DNA sequences and genes, there is a remarkable paucity of metrics to represent the genetic distance among diploid organisms. In our particular case, where the underlying data are based on multi-locus microsatellite genotypes, one ramet is characterized by a series of pairs of microsatellite repetitions at  $k$  loci, with  $k=7$  in our case.

More specifically, the genotype of a particular ramet, called  $A$ , is represented as:

$$A = (a_1, A_1)(a_2, A_2) \dots (a_k, A_k),$$

where  $a_i$  and  $A_i$  are the allele length (in number of nt) in both chromosomes at locus  $i$ .

Given a second ramet,  $B$ , with genotype

$$B = (b_1, B_1)(b_2, B_2) \dots (b_k, B_k),$$

we define a dissimilarity degree between  $A$  and  $B$  at locus  $i$  as:

$$d_i(A, B) = \min(|A_i - B_i| + |a_i - b_i|, |A_i - b_i| + |a_i - B_i|),$$

which provides a parsimonious (i.e., minimal) representation of the genetic distance, understood as the difference in allele length, between samples  $A$  and  $B$ . If we order the alleles at each locus in such a way that  $a_i < A_i$  and  $b_i < B_i$ , then the min function always select its first argument. We define *genetic distance* among ramets by adding up the contributions from each locus:

$$D(A, B) = \sum_{i=1}^k d_i,$$

which provides the degree of global dissimilarity degree between  $A$  and  $B$ . Since we have  $D(A, A) = 0$ , genetically identical individuals (clones) are at zero distance according to this definition.

To the best of our knowledge, the genetic distance metric  $D$  proposed here to characterize dissimilarities among diploid organisms has not been formally described as yet in the literature. It is, however (P. Meirmans, personal communication), the distance definition implemented for calculating distances among diploid organisms in the widely used genetic software GENOTYPE (7).

### Simulations

We performed computer simulations to explore the genetic distance between parents and offspring. We started with the ramets sampled in the meadow and generated new virtual ramets by allowing two classes of reproductive events: sexual reproduction within clones (i.e., selfing) or among genetically different parents (i.e., outcrossing). Such sexual reproduction was modeled by generating new multi-locus genotypes by randomly selecting, for each locus, one of the two microsatellite repeats present in each of the parents at that locus. In this work we focused on the ranges of inter-individual genetic distances generated within the population to underline the intra-population factors (clonality, mutation, mating system) that can account for such distances. We therefore calculated the distribution of genetic distances between offspring and their corresponding parents for each of the populations and reproductive modes (i.e., selfing and outcrossing). In addition, simulations of outcrossing events were performed over 12 generations and the mean distances between offspring and each set of ancestors present in the original meadow were computed. The resulting distances were characterized by their mean value across populations and the associated standard deviation.

### Network analysis

In mathematical terms, a network is represented by a graph. A graph is a pair of sets  $G = \{P, E\}$ , where  $P$  is a set of  $N$  nodes (here the ramets) and  $E$  is a set of edges connecting the nodes (here they are the links established among ramets at a genetic distance smaller than the threshold  $D_{th}$ ). Each edge connects only two nodes ( $P_i$  and  $P_j$ ), and therefore can be assigned a weight or length equal to the distance or degree of dissimilarity between them  $D(P_i, P_j)$ . Depending on the maximum distance ( $D_{th}$ ) allowed between two nodes for them to be connected, the range of possible networks is between a fully connected network (any distance is accepted, and therefore all individuals are connected), or a network in which only identical nodes are connected ( $D_{th}=0$ ). Here we chose to study population networks built by using as a threshold the average distance,  $\delta_{oc}$ , found between parents and offspring in the simulations performed to illustrate the pairwise genetic relationships in the meadows within a “one generation” path. We therefore allowed the network to be fragmented or partially fragmented into clusters (connected components), possibly illustrating the occurrence of sub-structure in the meadows analyzed. Inside a cluster, there is a path connecting any two nodes. On the contrary, there is no path connecting nodes belonging to different clusters. We define the quantity  $S$  as the size (number of nodes) of the biggest cluster in the network. We have  $S \leq N$ .

The degree of connectivity  $k_i$  of node  $P_i$  is defined as the number of nodes linked to it (i.e., the number of neighbor nodes). If each of these neighbors were connected with all the others, there would be  $E_i^{(max)} = k_i(k_i - 1)/2$  edges between them. The clustering coefficient  $C_i$  of node  $P_i$  is defined as:

$$C_i = \frac{2E_i}{k_i(k_i-1)},$$

where  $E_i$  is the number of edges that actually exist between these  $k_i$  neighbors of node  $P_i$ . The clustering coefficient of the whole network is the average of all individual clustering coefficients. Another important descriptor of the network as a whole is the *degree distribution*  $P(k)$ , defined as the proportion of nodes having degree  $k$ . The average degree  $\langle k \rangle$  may be derived from it.

The *path length* between any two nodes is defined as the minimal number of hops separating them. The diameter  $L$  of the network is the maximal path length present in the network. Finally, the density of links  $\rho$  is the ratio between the actual number of links present in the network and the number of links in a fully connected network [i.e.,  $N(N-1)/2$ ].

In this work we need to compare the networks observed with random networks having the same number of nodes and links. There are several ways to obtain a random network with a specific number of nodes and links. The standard random networks introduced by Erdős and Rényi (33) simply distribute randomly the links between the nodes. However, this algorithm produces its own degree of distribution. To avoid this effect, we have randomized the networks while keeping the observed degree of distribution. In particular, starting from the original network, we picked two links and permuted the end nodes as described in reference (27). By repeating this procedure, we obtained random networks with the original degree of distribution, but without correlations.

### Acknowledgements

This research was funded by a project of the BBVA Foundation (Spain), by a project and NETWORK (POCI/MAR/57342/2004) of the Portuguese Science Foundation (FCT) and CONOCES (fis2004-00953) of the Spanish MEC. S.A.H. was supported by a postdoctoral fellowship from FCT and the European Social Fund and A.F.R. by a post-doctoral fellowship of the Spanish Ministry of Education and Science.

### References

1. Wright, S. (1931) *Genetics* **16**, 97–159.
2. Hey, J. & Machado, C. A. (2003) *Nat. Rev. Genet.* **4**, 535–543.
3. Orive, M. E. (1993) *Theor. Popul. Biol.* **44**, 316–340.
4. Yonezawa, K., Ishii, T., & Nagamine, T. (2004) *Genetics* **166**, 1529–1539.
5. Fischer, M. & Van Kleunen, M. (2002) *Evol. Ecol.* **15**, 565–582.
6. Orive, M. E. (1995) *Am. Nat.* **145**, 90–108.
7. Meirmans, P. G. & Van Tienderen, P. H. (2004) *Mol. Ecol. Notes* **4**, 792–794.
8. Douhovnikoff, V. & Dodd, R. S. (2003) *Theor. Appl. Genet.* **106**, 1307–1315.
9. Posada, D. & Crandall, K. A. (2001) *Trends Ecol. Evol.* **16**, 37–45.
10. Excoffier, L. & Smouse, P. E. (1994) *Genetics* **136**, 343–359.
11. Templeton, A. R., Crandall, K. A., & Sing, C. F. (1992) *Genetics* **132**, 619–633.
12. Rueness, E. K., Stenseth, N. C., O'Donoghue, M., Boutin, S., Ellegren, H., & Jakobsen, K. S. (2003) *Nature* **425**, 69–72.
13. Cassens, I., Van Waerebeek, K., Best, P. B., Crespo, E. A., Reyes, J., & Milinkovitch, M. C. (2003) *Mol. Ecol.* **12**, 1781–1792.
14. Morrison, D. A. (2005) *Int. J. Parasitol.* **35**, 567–682.
15. Dyer, J. R. & Nason, J. D. (2004) *Mol. Ecol.* **13**, 1713–1727.
16. Proulx, S. R., Promislow, D. E. L., & Phillips, P. C. (2005) *Trends Ecol. Evol.* **20**, 345–353.
17. Dunne, J. A., Williams, R. J., & Martinez, N. D. (2002) *Proc. Natl. Acad. Sci. USA* **99**, 12917–12922.
18. Dunne, J. A., Williams, R. J., & Martinez, N. D. (2002) *Ecol. Lett.* **5**, 558–567.
19. Jeong, H., Mason, S. P., Barabási, A.-L., & Oltvai, Z. N. (2001) *Nature* **411**, 41–42.
20. Davidson, E., Sleeman, B. D., Rayner, A. D. M., Crawford, J. W., & Ritz, K. (2002) *Science* **295**, 1669–1678.
21. Van der Hulst, R. G. M., Mes, T. H. M., Falque, M., Stam, P., Den Nijs, J. C. M., & Bachmann, K. (2003) *Heredity* **90**, 326–335.
22. Arnaud-Haond, S., Alberto, F., Procaccini, G., Serrao, E. A., & Duarte, C. M. (2005) *J. Hered.* **96**, 1–8.
23. Hemminga, M. A. & Duarte, C. M. (2000) *Seagrass Ecology* (Cambridge University Press, Cambridge, UK).
24. Albert, R. & Barabási, A. L. (2002) *Rev. Mod. Phys.* **74**, 47–97.
25. Watts, D. J. & Strogatz, S. H. (1998) *Nature* **393**, 440–442.
26. Bowcock, A. M., Ruiz-Linares, A., Tomfohrde, J., Minch, E., Kidd, J. R., & Cavalli-Sforza, L. L. (1994) *Nature* **368**, 455–457.
27. Maslov, S. & Sneppen, K. (2002) *Science* **296**, 910–913.
28. Marbà, N., Duarte, C. M., Cebrian, J., Gallegos, M. E., Olesen, B., & SandJensen, K. (1996) *Mar. Ecol. Prog. Ser.* **137**, 203–213.
29. Moreno, D., Aguilera, P. A., & Castro, H. (2001) *Biol. Conserv.* **102**, 325–332.
30. Marba, N., Duarte, C. M., Diaz-Almela, E., Terrados, J., Alvarez, E., Martinez, R., Santiago, R., Garcia, E., & Grau, A. M. (2005) *Estuaries* **28**, 53–62.
31. Doyle, J. J. & Doyle, J. L. I. (1987) *Phytochem. Bull.* **11**, 11–15.
32. Alberto, F., Correia, L., Arnaud-Haond, S., Billot, C., Duarte, C. M., & Serrão, E. (2003) *Mol. Ecol. Notes* **3**, 253–255.
33. Erdős, P. & Rényi, A. (1959) *Publ. Math.* **6**, 290.

## Figure Captions

**Fig 1.** GDS: the distribution of genetic distances for two representative populations (a) Es Castell, which is a strictly clonal population ( $R=0.1$ ), and (b) Aqua Azzura 5, which is a non-clonal population ( $R=0.72$ ).

**Fig 2.** Circles:  $\langle GDS \rangle$ , the distribution of genetic distances averaged across sampled populations. The error bars indicate the SE for each bin. The square points (and corresponding error bars) were obtained from numerical simulations (see Methods) aimed at identifying mean ( $\pm SE$ ) genetic distances generated by different biological processes:  $\delta_c=0$  (clonal reproduction),  $\delta_m=6$  (somatic mutations),  $\delta_s=13.8\pm1.1$  (selfing, sexual reproduction between genetically identical individuals),  $\delta_{oc}$  (outcrossing, sexual reproduction between genetically different individuals):  $\delta_{oc}^{(1)}=24.0\pm1.2$ ,  $\delta_{oc}^{(2)}=29.4\pm1.5$ ,  $\delta_{oc}^{(4)}=34.0\pm1.8$  and  $\delta_{oc}^{(8)}=35.4\pm1.8$ . The upper index indicates the number of generations apart for which the distance has been measured. In the inset we show the same distribution on a log-linear scale. The straight line is a guide for the eye to highlight the exponential decay of the tail.

**Fig 3.** Solid line: cumulative distribution of genetic distances, obtained as the integral of the distribution shown in Fig. 2. We indicate the fraction of between-individual distances up to the values associated with different biological processes: mutation, selfing, and outcrossing of 1, 2, 4 and 8–12 generations. Inset: the whole range of genetic distances.

**Fig 4.** Network of genets for (a) Es Castell (Cabrera, Balearic Islands), (b) Cala Jonquet (Iberian Peninsula), (c) Rodalquilar (Iberian Peninsula), (d) Aqua Azzura (Sicily), (e) Roquetas (Iberian Peninsula) and (f) Playa Cavallets (Ibiza) after elimination of links representing genetic distances above the threshold  $D_{th}=\delta_{oc}^{(1)}$ . The node size is proportional to the number of identical constituent ramets.

**Fig 5a.** Supplementary material. We show the genetic diversity spectrum for each sampled meadow: (1) Aqua Azzura 3, (2) Aqua Azzura 5, (3) Addaia, (4) Amathous 3, (5) Amathous 5, (6) Ágios Nicolaos, (7) Calabardina, (8) Cala Giverola, (9) Cala Jonquet, (10) Campomanes, (11) Carboneras, (12) El Arenal, (13) Es Castell, (14) Es Pujols, (15) Es Calo de s'Oli, (16) Ses Illetes, (17) Cala Fornells, (18) La Fossa Calpe, (19) Las Rotes, and (20) Los Genoveces.

**Fig 5b.** (21) Magaluf, (22) Malta, (23) Marzamemi, (24) Es Port, (25) Paphos, (26) Playa Cavallets, (27) Port Lligat, (28) Porto Colom, (29) Punta Fanals, (30) Rodalquilar, (31) Roquetas, (32) Cala Santa Maria 13, (33) Cala Santa Maria 7, (34) Cala Torreta, (35) Torre de la Sal, and (36) Tunis.

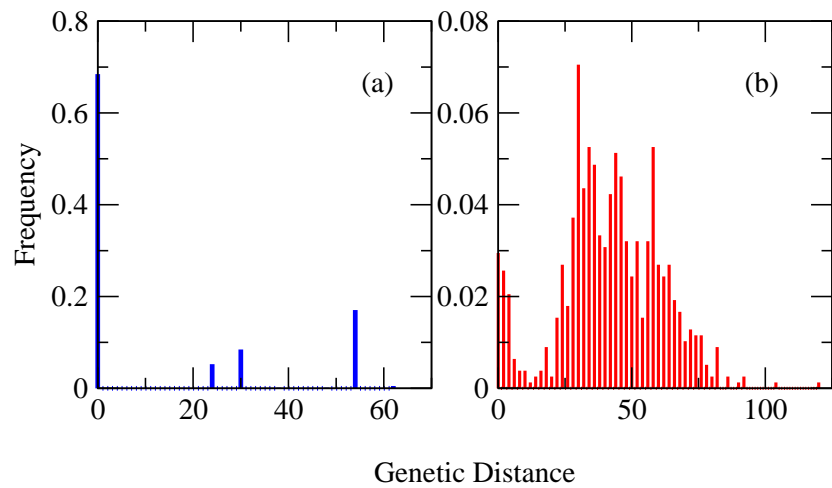


Figure 1: GDS: the distribution of genetic distances for two representative populations (a) Es Castell, which is a strictly clonal population ( $R=0.1$ ), and (b) Aqua Azzura 5, which is a non-clonal population ( $R=0.72$ ).

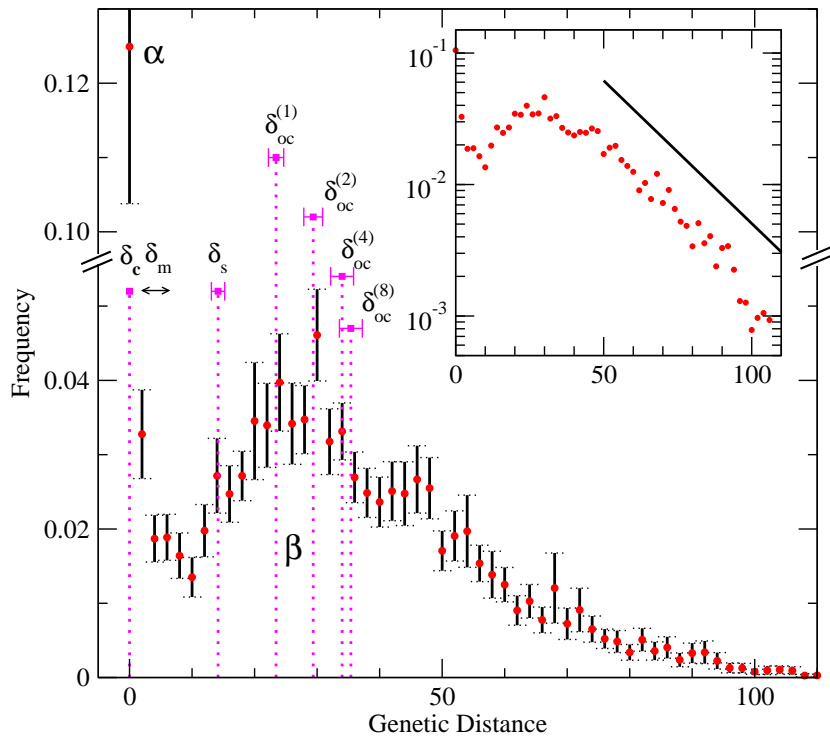


Figure 2: Circles:  $\langle \text{GDS} \rangle$ , the distribution of genetic distances averaged across sampled populations. The error bars indicate the SE for each bin. The square points (and corresponding error bars) were obtained from numerical simulations (see Methods) aimed at identifying mean ( $\pm \text{SE}$ ) genetic distances generated by different biological processes:  $\delta_c = 0$  (clonal reproduction),  $\delta_m = 6$  (somatic mutations),  $\delta_s = 13.8 \pm 1.1$  (selfing, sexual reproduction between genetically identical individuals),  $\delta_{oc}$  (outcrossing, sexual reproduction between genetically different individuals):  $\delta_{oc}^{(1)} = 24.0 \pm 1.2$ ,  $\delta_{oc}^{(2)} = 29.4 \pm 1.5$ ,  $\delta_{oc}^{(4)} = 34.0 \pm 1.8$  and  $\delta_{oc}^{(8)} = 35.4 \pm 1.8$ . The upper index indicates the number of generations apart for which the distance has been measured. In the inset we show the same distribution on a log-linear scale. The straight line is a guide for the eye to highlight the exponential decay of the tail.

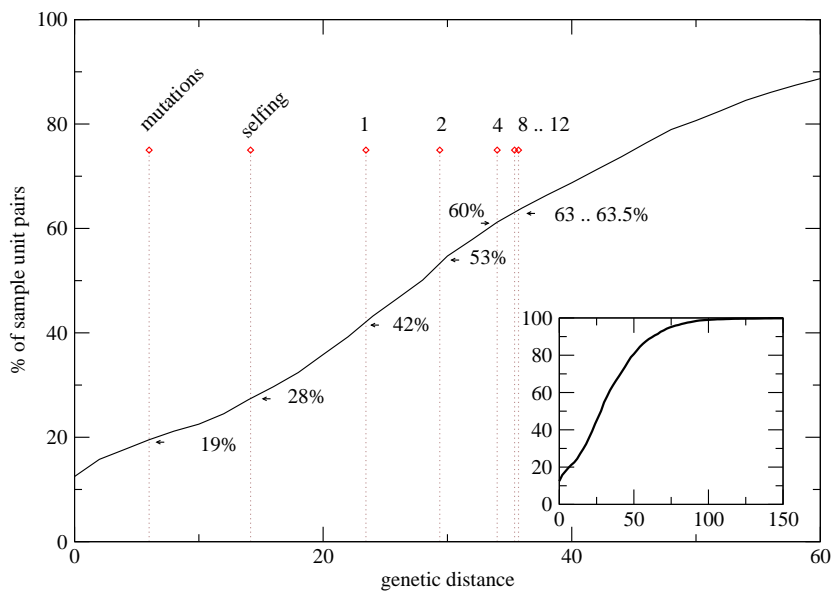
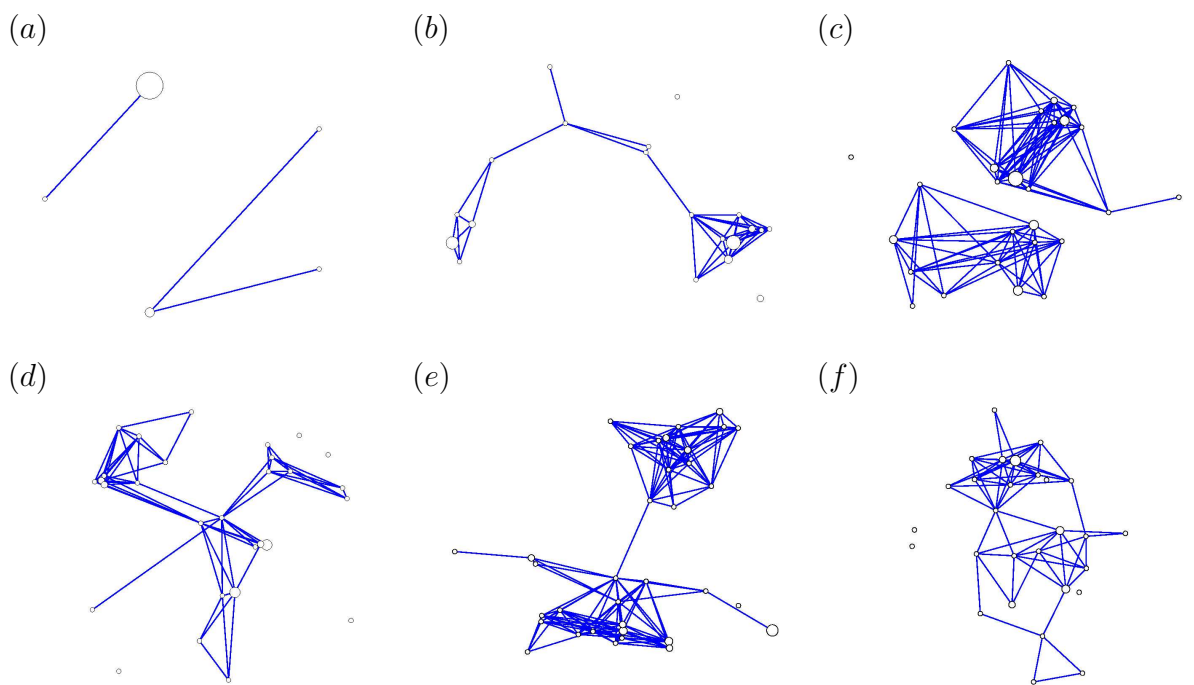
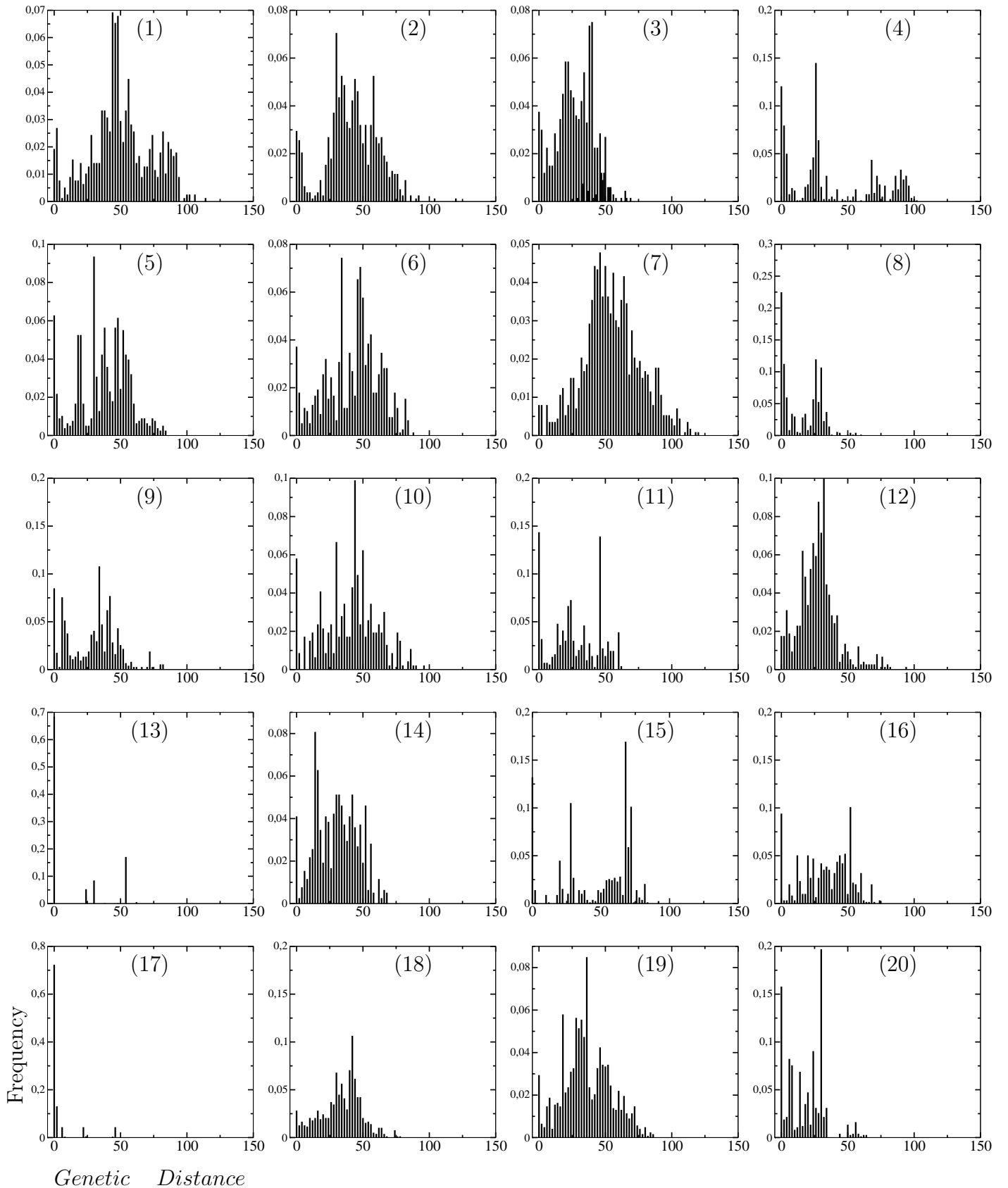


Figure 3: Solid line: cumulative distribution of genetic distances, obtained as the integral of the distribution shown in Fig. 2. We indicate the fraction of between-individual distances up to the values associated with different biological processes: mutation, selfing, and outcrossing of 1, 2, 4 and 812 generations. Inset: the whole range of genetic distances.



**Fig 4.** Network of genets for (a) Es Castell (Cabrera, Balearic Islands), (b) Cala Jonquet (Iberian Peninsula), (c) Rodalquilar (Iberian Peninsula), (d) Aqua Azzura (Sicily), (e) Roquetas (Iberian Peninsula) and (f) Playa Cavallets (Ibiza) after elimination of links representing genetic distances above the threshold  $D_{th}=\delta_{oc}^{(1)}$ . The node size is proportional to the number of identical constituent ramets.



**Fig 5a.** Supplementary material. We show the genetic diversity spectrum for each sampled meadow: (1) Aqua Azzura 3, (2) Aqua Azzura 5, (3) Addaia, (4) Amathous 3, (5) Amathous 5, (6) Agios Nicolaos, (7) Calabardina, (8) Cala Giverola, (9) Cala Jonquet, (10) Campomanes, (11) Carboneras, (12) El Arenal, (13) Es Castell, (14) Es Pujols, (15) Es Calo de s'Oli, (16) Ses Illetes, (17) Cala Fornells, (18) La Fossa Calpe, (19) Las Rotes, and (20) Los Genoveces.

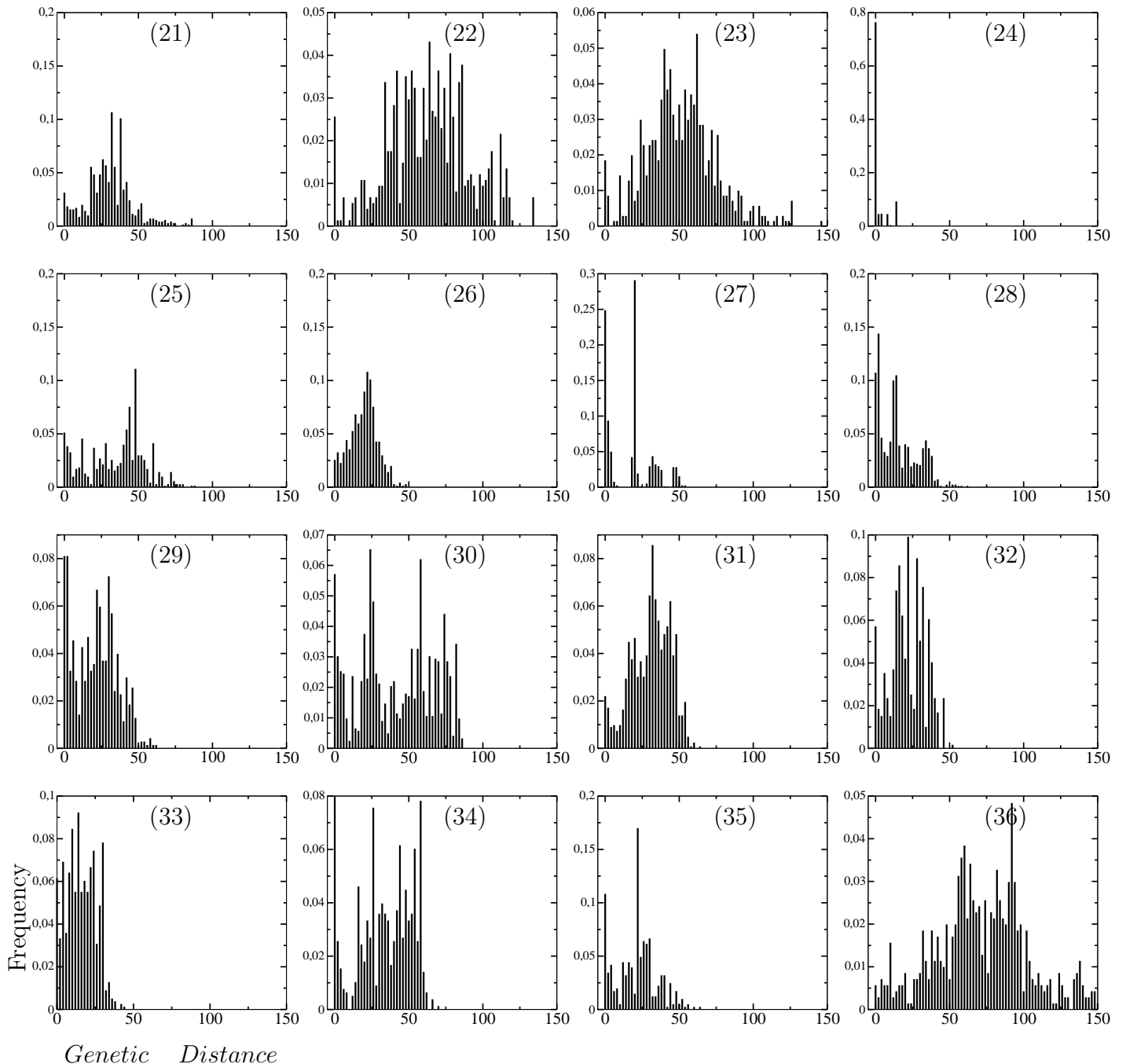


**Fig 5b.** (21) Magaluf, (22) Malta, (23) Marzamemi, (24) Es Port, (25) Paphos, (26) Playa Cavalllets, (27) Port Lligat, (28) Porto Colom, (29) Punta Fanals, (30) Rodalquilar, (31) Roquetas, (32) Cala Santa Maria 13, (33) Cala Santa Maria 7, (34) Cala Torreta, (35) Torre de la Sal, and (36) Tunis.

|                     | <i>G</i> | <i>S</i> | <i>C</i> | <i>L</i> | Cr   | Lr   | $\langle k \rangle$ | $\rho$ |
|---------------------|----------|----------|----------|----------|------|------|---------------------|--------|
| Acqua Azzura 3      | 31       | 28       | 0.80     | 3.13     | 0.22 | 2.17 | 4.71                | 0.16   |
| Acqua Azzura 5      | 29       | 25       | 0.78     | 2.43     | 0.26 | 2.01 | 4.76                | 0.17   |
| Addaia              | 25       | 17       | 0.72     | 1.64     | 0.41 | 1.91 | 5.60                | 0.23   |
| Amathous 3          | 18       | 11       | 0.77     | 1.45     | 0.33 | 1.86 | 4.67                | 0.27   |
| Amathous 5          | 25       | 24       | 0.73     | 3.14     | 0.29 | 2.19 | 4.56                | 0.19   |
| Agios Nicolaos      | 28       | 18       | 0.81     | 2.41     | 0.27 | 2.13 | 5.50                | 0.20   |
| Calabardina         | 40       | 40       | 0.62     | 3.44     | 0.19 | 2.25 | 5.90                | 0.15   |
| Cala Giverola       | 17       | 10       | 0.84     | 1.22     | 0.70 | 1.76 | 4.35                | 0.27   |
| Cala Jonquet        | 20       | 18       | 0.79     | 2.95     | 0.37 | 1.89 | 4.60                | 0.24   |
| Campomanes          | 22       | 12       | 0.66     | 1.77     | 0.25 | 2.18 | 4.00                | 0.19   |
| Carboneras          | 16       | 16       | 0.78     | 1.75     | 0.75 | 1.49 | 8.50                | 0.57   |
| El Arenal           | 32       | 27       | 0.76     | 2.74     | 0.27 | 2.11 | 5.25                | 0.17   |
| Es Castell          | 05       | 03       | 0.00     | 1.33     | 0.00 | 1.33 | 1.20                | 0.30   |
| Es Pujols           | 27       | 24       | 0.74     | 2.76     | 0.57 | 1.97 | 5.70                | 0.22   |
| Es Calo de s'Oli    | 15       | 07       | 0.73     | 1.14     | 0.49 | 1.98 | 2.80                | 0.20   |
| Ses Illetes         | 21       | 20       | 0.78     | 2.62     | 0.36 | 1.82 | 5.52                | 0.28   |
| Cala Fornells       | 05       | 03       | 1.00     | 1.00     | 1.00 | 1.00 | 1.20                | 0.30   |
| La Fossa Calpe      | 31       | 29       | 0.63     | 2.76     | 0.24 | 2.08 | 5.55                | 0.18   |
| Las Rotes           | 34       | 21       | 0.75     | 1.98     | 0.20 | 2.25 | 4.65                | 0.14   |
| Los Genoveces       | 14       | 13       | 0.86     | 1.45     | 0.86 | 1.34 | 7.71                | 0.59   |
| Magaluf             | 26       | 18       | 0.64     | 1.88     | 0.39 | 2.11 | 4.46                | 0.18   |
| Malta               | 29       | 24       | 0.67     | 2.19     | 0.33 | 1.89 | 5.24                | 0.19   |
| Marzamemi           | 31       | 28       | 0.63     | 2.48     | 0.39 | 2.07 | 5.61                | 0.19   |
| Es Port             | 05       | 05       | 0.90     | 1.10     | 0.90 | 1.10 | 3.60                | 0.90   |
| Paphos              | 26       | 17       | 0.74     | 1.65     | 0.43 | 1.95 | 6.54                | 0.26   |
| Playa Cavallers     | 28       | 24       | 0.63     | 2.45     | 0.30 | 1.97 | 4.86                | 0.18   |
| Port Lligat         | 12       | 07       | 0.95     | 1.10     | 0.43 | 1.59 | 4.17                | 0.38   |
| Porto Colom         | 21       | 16       | 0.83     | 1.42     | 0.75 | 1.55 | 7.62                | 0.38   |
| Punta Fanals        | 26       | 26       | 0.70     | 2.06     | 0.48 | 1.83 | 7.54                | 0.30   |
| Rodalquilar         | 27       | 14       | 0.84     | 1.32     | 0.37 | 1.75 | 8.22                | 0.32   |
| Roquetas            | 35       | 34       | 0.79     | 2.47     | 0.33 | 1.86 | 8.74                | 0.26   |
| C.Sta.Maria 13      | 20       | 19       | 0.73     | 2.37     | 0.43 | 1.79 | 5.50                | 0.29   |
| C.Sta.Maria 7       | 22       | 16       | 0.66     | 1.74     | 0.61 | 1.82 | 4.91                | 0.23   |
| Cala Torreta        | 21       | 10       | 0.75     | 1.84     | 0.13 | 2.37 | 3.33                | 0.17   |
| Torre de la Sal     | 15       | 13       | 0.71     | 1.64     | 0.58 | 1.64 | 4.93                | 0.35   |
| Tunis               | 34       | 30       | 0.77     | 2.80     | 0.28 | 2.15 | 5.41                | 0.16   |
| Xilxes              | 12       | 05       | 0.47     | 1.80     | 0.08 | 2.37 | 1.50                | 0.14   |
| $\langle x \rangle$ | 22.84    | 18.16    | 0.73     | 2.04     | 0.41 | 1.88 | 5.11                | 0.27   |
| $\sigma$            | 8.54     | 8.82     | 0.16     | 0.65     | 0.23 | 0.32 | 1.77                | 0.15   |
| $\min(x)$           | 5.00     | 3.00     | 0.00     | 1.00     | 0.00 | 1.00 | 1.20                | 0.14   |
| $\max(x)$           | 40.00    | 40.00    | 1.00     | 3.44     | 1.00 | 2.37 | 8.74                | 0.90   |

**Table 1.** Summary of properties measured for population genetic networks of genets (non-similar ramets) at  $D_{th}=\delta_{oc}$ .  $G$  is the number of genets present in the meadow,  $S$  stands for the size of major connected components,  $C$  for the clustering,  $L$  for the diameter, Cr and Lr for the clustering and diameter after random rewiring,  $\langle k \rangle$  for the mean degree of connectivity and  $\rho$  for the link density.

|                          | Locality             | Latt.        | Long.       | SUs | R    |
|--------------------------|----------------------|--------------|-------------|-----|------|
| SPAIN (Iberic Peninsula) |                      |              |             |     |      |
|                          | Roquetas             | 36° 43.26'N  | 2° 37.09'W  | 50  | 0.69 |
|                          | Rodalquilar          | 36° 51.21'N  | 2° 00.53W   | 50  | 0.53 |
|                          | Los Genoveces        | 36° 44.40'N  | 2° 07.02W   | 39  | 0.34 |
|                          | Carboneras           | 36° 69,61'N  | 1° 53.20'W  | 48  | 0.32 |
|                          | Calabardina          | 37° 26.00'N  | 1° 30.00'W  | 48  | 0.88 |
|                          | Campomanes           | 38° 37.54' N | 0° 0.57'E   | 31  | 0.7  |
|                          | Torre de la Sal      | 40° 8.13' N  | 0° 10.72'E  | 39  | 0.5  |
|                          | El Arenal            | 38° 38.37' N | 0° 3.06'E   | 39  | 0.86 |
|                          | La Fossa             | 38° 33.59'N  | 0° 4.56'E   | 40  | 0.77 |
|                          | Xilxes               | 39° 45.13' N | 0° 8.07'E   | 32  | 0.35 |
|                          | Las Rotes            | 38° 50.03' N | 0° 8.56'E   | 50  | 0.73 |
|                          | Fanals               | 41° 41.58'N  | 2° 50.56'E  | 38  | 0.68 |
|                          | Cala Giverola        | 41° 44.15'N  | 2° 57.37'E  | 38  | 0.43 |
|                          | Cala Jonquet         | 42° 18.19'N  | 3° 17.36'E  | 39  | 0.50 |
|                          | Port Lligat          | 42° 17.61'N  | 3° 17.58'E  | 40  | 0.28 |
| SPAIN (Balearic Islands) |                      |              |             |     |      |
| Ibiza                    | Playa Cavallets      | 38° 50.99'N  | 1° 24.25'E  | 38  | 0.73 |
| Formentera               | Es Calo de s'Oli     | 38° 43.49'N  | 1° 24.16'E  | 40  | 0.36 |
|                          | Cala Torreta         | 38° 47.45'N  | 1° 25.18'E  | 40  | 0.51 |
|                          | Ses Illetes          | 38° 45.37'N  | 1° 25.83'E  | 36  | 0.60 |
|                          | Es Pujols            | 38° 43.74'N  | 1° 27.27'E  | 40  | 0.67 |
| Cabrera                  | Es Castell           | 39° 9.16'N   | 2° 55.83'E  | 40  | 0.10 |
|                          | Es Port              | 39° 8.81'N   | 2° 55.86'E  | 40  | 0.10 |
|                          | Cala Sta. María 13 m | 39° 9.07'N   | 2° 56.92'   | 35  | 0.56 |
|                          | Cala Sta. María 7 m  | 39° 9.00'N   | 2° 56.96'E  | 40  | 0.54 |
| Mallorca                 | Magaluf              | 39° 30.25'N  | 2° 32.59'E  | 38  | 0.68 |
|                          | Porto Colom          | 39° 25.05'N  | 3° 16.18'E  | 41  | 0.50 |
| Menorca                  | Cala Fornells        | 40° 03.39'N  | 4° 08.26'E  | 40  | 0.10 |
|                          | Addaia               | 40° 00.97'N  | 4° 12.42'E  | 37  | 0.67 |
| TUNISIA                  | Tunisia              | 36° 46.00'N  | 10° 19.00'E | 40  | 0.85 |
| MALTA                    | Malta                | 35° 51.00'N  | 14° 35.00'E | 39  | 0.74 |
| ITALY( Sicily)           | Acqua Azzurra 3      | 36° 42.71'N  | 15° 8.44'E  | 40  | 0.77 |
|                          | Acqua Azzurra 5      | 36° 43.31'N  | 15° 8.48'E  | 40  | 0.72 |
|                          | Marzamemi            | 36° 43.29'N  | 15° 0.49'E  | 38  | 0.81 |
| GREECE                   | Agios Nicolaos       | 37° 42.97'N  | 23° 55.62'E | 40  | 0.69 |
| CYPRUS                   | Amathous 3           | 34° 41.96'N  | 33° 12'00'E | 40  | 0.44 |
|                          | Amathous 5           | 34° 42.02'N  | 33° 12.99'  | 40  | 0.62 |
|                          | Paphos               | 34° 43.54'N  | 32° 26.23'E | 38  | 0.68 |

**Table 2.** Supplementary material. Sampling details: country, locality, approximate GPS coordinates, number of sampling units collected (SUs), genotype diversity ( $R$ ).